Neurobiology of Aging 34 (2013) 1717–1727

Contents lists available at SciVerse ScienceDirect

Neurobiology of Aging

journal homepage: www.elsevier.com/locate/neuaging

Modulation of DNA base excision repair during neuronal differentiation

Peter Sykora [a], Jenq-Lin Yang [a,b,1], Leslie K. Ferrarelli [a], Jingyan Tian [a], Takashi Tadokoro [a], Avanti Kulkarni [c], Lior Weissman [a], Guido Keijzers [a,d], David M. Wilson III [a], Mark P. Mattson [b], Vilhelm A. Bohr [a,*]

[a] Laboratory of Molecular Gerontology, National Institute on Aging/National Institutes of Health (NIA/NIH), Baltimore, MD, USA
[b] Laboratory of Neurosciences, National Institute on Aging/National Institutes of Health (NIA/NIH), Baltimore, MD, USA
[c] Roche Palo Alto, LLC, Palo Alto, CA, USA
[d] Center for Healthy Aging, Faculty for Health Sciences, University of Copenhagen, Denmark

ARTICLE INFO

Article history:
Received 1 April 2012
Received in revised form 21 December 2012
Accepted 22 December 2012
Available online 1 February 2013

Keywords:
BER
Differentiation
DNA repair
Postmitotic
Aging
Neuron
DNA damage

ABSTRACT

Neurons are terminally differentiated cells with a high rate of metabolism and multiple biological properties distinct from their undifferentiated precursors. Previous studies showed that nucleotide excision DNA repair is downregulated in postmitotic muscle cells and neurons. Here, we characterize DNA damage susceptibility and base excision DNA repair (BER) capacity in undifferentiated and differentiated human neural cells. The results show that undifferentiated human SH-SY5Y neuroblastoma cells are less sensitive to oxidative damage than their differentiated counterparts, in part because they have robust BER capacity, which is heavily attenuated in postmitotic neurons. The reduction in BER activity in differentiated cells correlates with diminished protein levels of key long patch BER components, flap endonuclease-1, proliferating cell nuclear antigen, and ligase I. Thus, because of their higher BER capacity, proliferative neural progenitor cells are more efficient at repairing DNA damage compared with their neuronally differentiated progeny.

Published by Elsevier Inc.

1. Introduction

Neurons are highly differentiated nondividing cells that exhibit electrical excitability, a high metabolic rate, and abundant transcriptional activity. The high metabolic activity in these cells generates relatively large amounts of reactive oxygen species (ROS) that can damage lipids, proteins, and DNA. Unrepaired ROS-induced oxidative DNA damage in the nuclear and mitochondrial DNA of neurons can lead to cell death and contribute to aging and neurodegeneration.

Base excision DNA repair (BER) is the major pathway that repairs oxidative lesions, alkylated bases, single-strand breaks (SSBs) and abasic sites in nuclear and mitochondrial DNA (Englander, 2008; Martin, 2008). BER involves the sequential action of multiple enzymes, typically starting with the recognition and removal of an inappropriate base by a DNA glycosylase (Krokan et al., 1997). Glycosylases excise the damaged base forming an abasic site, which is primarily processed by an apurinic/apyrimidinic endonuclease (APE1). APE1 incises the sugar phosphate backbone at the abasic site generating a 1-nucleotide SSB. In short patch BER (SP-BER), the gap is filled by DNA polymerase β (Pol β) and, after 5′-terminal processing by Pol β, the nick is ligated by DNA ligase III. Other 3′ and 5′ terminal blocking groups are also resolved before ligation by BER-related factors such as aprataxin, polynucleotide kinase phosphatase, and tyrosyl DNA phosphodiesterase 1 (Frosina et al., 1996; Raymond et al., 2005; Takahashi et al., 2007; Whitehouse et al., 2001). Long patch BER (LP-BER), a subpathway of BER that engages several replication-associated proteins, involves strand-displacement synthesis and 5′-flap processing, often necessary to cope with complex 5′-termini. In this process, Pol β or DNA polymerase delta/epsilon (Pol δ/ε), flap endonuclease-1 (FEN-1), proliferating cell nuclear antigen (PCNA), and DNA ligase I coordinately resynthesize 2–10 nucleotides, displace the downstream strand, cleave away the 5′-flap that harbors the blocking group, and seal the remaining nick (Frosina et al., 1996).

Previous findings suggest that terminally differentiated muscle cells express very low levels of DNA ligase I and ligase III/XRCC1 (Narciso et al., 2007), leading to an impairment of both short and long patch BER in the myotubes. Hildrestrand et al. suggested that 8-oxoguanine glycosylase (OGG1) protein levels were lower in fully differentiated neurospheres than in undifferentiated neurospheres

* Corresponding author at: Laboratory of Molecular Gerontology, National Institute on Aging/National Institutes of Health (NIA/NIH), 251 Bayview Blvd, Ste 100, Room 6B133, Baltimore, MD 21224, USA. Tel.: +1 410 558 8162; fax: +1 410 558 8157.
E-mail addresses: bohrv@grc.nia.nih.gov, vbohr@nih.gov (V.A. Bohr).
[1] Current affiliation: Center for Translational Research in Biomedical Sciences, Kaohsiung Chang Gung Memorial Hospital, Kaohsiung, Taiwan.

0197-4580/$ – see front matter Published by Elsevier Inc.
http://dx.doi.org/10.1016/j.neurobiolaging.2012.12.016

(Hildrestrand et al., 2007), whereas Linn et al. reported that APE1 activity, but not Pol β and uracil DNA glycosylase (UDG) activities, were higher in differentiated neuroblastoma cells (Jensen and Linn, 1988). Additional studies suggest that expression of DNA repair proteins might vary in both a species- and tissue-specific manner (Aprelikova and Tomilin, 1982; Haug et al., 1998).

In the present study, we investigated BER capacity in undifferentiated and neuronally differentiated human SH-SY5Y neuroblastoma cells. DNA damage and cell viability were examined in differentiated and undifferentiated cells treated with hydrogen peroxide or methyl methane sulfonate (MMS), and the protein levels and enzyme activities of several BER factors were quantified. We report here that differentiated cells are more susceptible to DNA damage induced by oxidative stress, but not alkylating agents. This heightened sensitivity correlates with a dramatic decrease in BER components, potentially leading to the accumulation of a subset of oxidative DNA lesions in differentiated cells.

2. Methods

2.1. Cell culture and differentiation

The human neuroblastoma cell line SH-SY5Y (obtained from American Type Culture Collection) maintained in regular Dulbecco's Modified Eagle Medium (DMEM) (Invitrogen) with 10% fetal bovine serum, and 1% penicillin-streptomycin in 5% CO_2 at 37 °C. Mitotic SH-SY5Y cells are able to differentiate into postmitotic neuronal-like cells when cultured in medium with reduced serum levels and treatment with retinoic acid (Kulkarni et al., 2008). In the present study the postmitotic state was achieved by treating cells with 10 μM retinoic acid for 5 days followed by reseeding of the cells to polyethyleneimine (PEI)-coated Petri dishes in serum-free DMEM containing 10 ng/mL brain derived neurotrophic factor (BDNF; Chemicon) for another 5 days.

2.2. Immunocytochemistry

The cells were fixed in 4% paraformaldehyde (in phosphate buffered saline [PBS]) and incubated with lysis buffer (0.5% Triton X-100, 100 mM glycine, 1% bovine serum albumin [BSA], 0.7 mM ethylenediaminetetraacetic acid [EDTA]) for 10 minutes on ice. After lysis the cells were incubated with blocking buffer (10% donkey serum, 0.01% sodium azide in PBS). The blocked cells were incubated with primary antibodies, Tuj1 (1:250; Sigma-Aldrich) or microtubule associated protein 2 (MAP2; 1:500, Chemicon), for 60 minutes at 37 °C. The samples were then briefly rinsed with wash buffer (0.05% Triton X-100 in PBS) 3 times for 5 minutes at room temperature before incubation with conjugated secondary antibody (Alexa 488; 1:1000; donkey anti-mouse; Invitrogen) for 60 minutes at 37 °C. After incubation the cells were washed with PBS (3 times for 5 minutes) and mounted with Prolong Gold containing 4′,6′- diamidino-2-phenylindole (a nuclear marker from Invitrogen). Images of immunostained cells were captured using a Nikon Eclipse TE2000 confocal microscope system running Volocity software (Perkin Elmer).

2.3. Measurement of cell viability

Cells (10,000 per well in a 96-well plate coated with PEI) were treated in triplicate with MMS (0.1–4 mM) for 60 minutes or hydrogen peroxide (0.01–1 mM) for 40 minutes in standard growth medium for replicating SH-SY5Y cells or in serum-free/BDNF medium for differentiated cells. After treatment, cells were refreshed with 200 μL of respective medium and incubated at 37 °C for 24 hours. Viability was quantified using the lactate dehydrogenase (LDH) cytotoxicity detection kit (Roche Applied Science, Indianapolis, IN, USA) by incubating 100 μL of media from each well with 100 μL of reaction mixture for 15 minutes at room temperature and reading on a Bio-Rad microplate spectrophotometer. Cytotoxicity was proportional to the absorbance (OD) at 492 nm (reference wavelength 690 nm) as a measure of LDH activity released from damaged cells into the media and was calculated against that measured for untreated controls. Maximal cellular LDH release was determined by treating cells with 1% Triton X-100 for 60 minutes; OD values greater than this level were excluded.

The WST-8 assay was also used to assess cytotoxicity. Cells (20,000 per well in a 96-well plate coated with PEI) were treated in triplicate with MMS (0.02–2 mM) or hydrogen peroxide (0.01–1 mM) for 4 hours at 37 °C in 100 μL standard growth medium for replicating SH-SY5Y cells or serum-free/BDNF medium for differentiated cells. Viability was quantified using the WST-8 cytotoxicity assay kit (Dojindo Molecular Technologies, Rockville, MD, USA) by incubating wells in 10 μL Cell Counting Kit- 8 (CCK) solution for 2 hours at 37 °C and reading on a Bio-Rad microplate spectrophotometer. Cell viability was directly proportional to the OD at 450 nm as a measure of dehydrogenase activity in viable cells and was calculated against that measured for untreated controls.

2.4. Alkali single-cell gel electrophoresis (comet assay)

Alkali single-cell gel electrophoresis was performed as described previously (Morris et al., 1999). Cells were washed with PBS before medium containing 50 μM H_2O_2 was added and cultures were incubated for 40 minutes at 37 °C or treated with 100 μM MMS for 60 minutes at 37 °C. After the chemical treatment, cells were washed once with fresh DMEM. Cells were prepared at 0 hours, with and without treatment, and 6 and 24 hours after treatment. Briefly, cells were rinsed in PBS, and approximately 10,000 cells were mixed with 75 μL of low melt point agarose and spread onto an agarose-coated glass slide. After the low melt point agarose had set, the coverslip was removed, another 75 μL of low melt point agarose was added, and the slide was placed on a chilled aluminum tray for 5 minutes. The slide was incubated in lysis buffer (2.5 M NaCl, 100 mM EDTA, 10 mM Tris, and 1% Triton X-100) for at least 4 hours then washed with neutralization buffer (0.4 M Tris, pH 7.4), followed by a 10-minute incubation with buffer (10 mM 4-(2-hydroxyethyl)-1-iperazineethanesulfonic acid (HEPES)-KOH, 100 mM KCl, 10 mM EDTA, 0.1 mg/mL BSA; pH 7.4). For enzymatic treatments, slides were incubated with formamidopyrimidine DNA glycosylase (New England Biolabs) or mouse 3-methyladenine DNA glycosylase (Aag; Trevigen) at 37 °C for 60 minutes. Formamidopyrimidine DNA glycosylase treatment was used on samples exposed to hydrogen peroxide and related controls, and Aag treatment was used on MMS-exposed sets and related controls. The enzyme-treated slides were rinsed with alkali buffer (300 mM NaOH and 1 mM EDTA; pH 12.1) for 20 minutes to denature the DNA. Electrophoresis was performed and the slides dehydrated in 100% ethanol for 5 minutes before staining with ethidium bromide (10 ng/mL). Images of nuclei were acquired under fluorescence illumination using a Zeiss Axiovert microscope, and images were analyzed using Komet 5.5 software (Kinetic Imagine). Statistical analysis was carried out using Graph Pad Prism software version 6.01, and statistical significance was assessed by comparing corresponding undifferentiated and differentiated data sets using Student *t* test.

2.5. BER activities

Cells were washed with PBS, centrifuged, and the cell pellets were used immediately for extraction or stored at −80 °C for future

use. Total protein was extracted by incubating the cell pellet in Radioimmunoprecipitation assay buffer (RIPA) buffer with protease inhibitors for 30 minutes at 4 °C, and the lysate was then briefly sonicated on ice (3 times for 10 seconds at 10% power) using a Branson sonicator then spun down at 10,000*g* at 4 °C for 30 minutes to remove cellular debris and DNA. Protein levels were quantified using the bicinchoninic acid method using bovine serum albumin as a known concentration standard. Extracts were used fresh or aliquoted and stored at −80 °C. All oligonucleotide DNA substrates used to measure various BER activities have been used extensively by our group and others, and are listed in Table 1. The SP-BER activity assay was used to measure polymerase incorporation and total ligation activity. The assay was initially performed using varying concentrations of protein extract. This preliminary step was conducted to identify the amount of protein that gave the least substrate degradation but still had detectable activity (not shown). The quantitative assay was then run using increasing incubation times, with only time points determined to be in the linear phase of the experiment subsequently used for further quantitative analysis. Experiments to assess the rate limiting step included the enzyme T4 ligase (Roche) and Pol β was also used as a positive control. More detailed methods regarding the activity assays are described in previous studies (Weissman et al., 2007, 2009).

2.6. Immunoblot analysis

Proteins were separated by sodium dodecyl sulfate-polyacrylamide gel electrophoresis, and transferred to a (polyvinylidene fluoride) membrane. After blocking in 5% nonfat milk protein in Tris buffered saline with 0.01% Tween-20, the membrane was exposed to 1 of the following primary antibodies; XRCC1 (1:500; Abcam), UDG (1:200; Santa Cruz), OGG1 (1:200; Santa Cruz), DNA ligase III (LIGIII) (1:500; BD Bioscience Technology), APE1 (1:1000; Imgenex), Pol β (1:500; Abcam), PCNA (1:2000; Santa Cruz), DNA ligase I (LIGI) (1:500; Santa Cruz), FEN-1 (1:250; Abcam), Pol ε (1:250; Abcam), glyceraldehyde 3-phosphate dehydrogenase (GAPDH) (1:1000; Abcam), and HSP60 (1:500; Abcam). β-Actin was used as a loading and transfer control (1:5000; Sigma-Aldrich). Secondary antibodies were as follows: anti-mouse (1:5000; Vector Laboratories), anti-goat (1:10,000; Vector Laboratories), and anti-rabbit (1:5000; Perkin Elmer).

Table 1
Combinations of oligonucleotides used to test the various BER activities

Activity	Substrate
8-oxo-G incision	5′-GAA CTG T(O)A GAC TGA T 3′-GCT GAC A C T GAA CTG ACG ACT A
Uracil incision	5′-ATA GG(U) CGG ATC AAG ATT 3′-TAT CC (G or A) GCC GAA TAA
AP incision	5′-GAA CTG T (F) A GAC TGA T 3′-GCT GAC A C T GAA CTG ACG ACT A
Incorporation	5′-CTG CTG ( )GT ACG GAT CGG C 3′-GAC GTC GAC GCA GCC G
Nick (ligation)	5′-TCC GTT GAA GCC TGC TTT GAC ATA CTA ACT TGA GCG AAA CGG-T-3′ 3′-T-ACG CAA CTT CGG ACG AAA CTG TAT GAT TGA ACT CGC TTT GCC-5′
BER (incorporation and ligation)	5′-TCC GTT GAA GCC TGC TTT ( )AC ATA CTA ACT TGA GCG AAA CGG-T-3′ 3′-T-ACG CAA CTT CGG ACG AAA CTG TAT GAT TGA ACT CGC TTT GCC-5′
LP-BER	5′-GTC CAC CCG ACG CCA CCT CCT GCC TTC AAT GTG CTG ( ) GAT CCT ACA ACC AAG ACG AAT TCC GGA TAC GAC GGC CAG TGC CGA CCG TGC CAG CCT AAA TTT CAA TCC ACC C-3′ 3′-CAG GTG GGC TGC GGT GGA GGA CGG AAG TTA CAC GAC C CTA GGA TGT TGG TTC TGC TTA AGG CCT ATG CTG CCG GTC ACG GCT GGC ACG GTC GGA TTT AAA GTT AGG TGG G-5′

Key: BER, base excision DNA repair; LP-BER, long patch BER.

2.7. LP-BER assay

LP-BER was measured using a substrate specific for only this repair activity. The substrate used a 110 mer backbone that has a biotin group on both ends (a gift from Dr Bambara, University of Rochester, Rochester, NY, USA). Annealed to the backbone is an unlabeled 36 mer and a 73 mer that has a 5′-tetrahydrofuran blocking group and a 3′-P^{32} end label. Before use, the annealed substrate was incubated with streptavidin for 30 minutes at 4 °C; this molecule forms a strong noncovalent bond with the biotin blocking both ends of the substrate. When the substrate is in this blocked conformation, PCNA must be loaded onto the substrate and cannot simply slide on or off (Jonsson et al., 1998). LP-BER activity was measured in total protein extracts (described earlier in this report) from differentiated and undifferentiated cells.

The repair reactions were assembled in a 20-μL volume. Depending on the assay conducted, either the protein concentration or incubation time was varied. For protein concentration-dependent reactions, between 0.5 and 2 μg of total protein extract was added to a reaction containing 50 fmol end-labeled substrate, 10 mM adenosine-5′-triphosphate [ATP], 10 μM deoxyribonucleotides [dNTPs], 20 ng DNA (λ), in reaction buffer (50 mM Tris-HCL, pH 8, 10 mM KCl, 10 mM $MgCl_2$, 1 mM dithiothreitol, and 1% glycerol) as described by Wei and Englander (2008). The reaction was carried out at 37 °C for 30 minutes, terminated with stopping buffer (30 mM Tris-HCL pH 8, 30 mM EDTA pH 8, 30% glycerol, 0.9% sodium dodecyl sulfate, 0.05% bromophenol blue), and heating at 95 °C for 5 minutes. Reaction products were separated in a 15% urea-acrylamide gel, at 15 W for 120 minutes. The gel products were quantitated using a GE Typhoon phosphoimager. This reaction was also carried out using varied incubation times between 15 minutes and 90 minutes under the identical conditions as described previously; for the SP-BER assay, this approach allowed us to first identify an amount of protein extract that gave clean reproducible results, and then using this amount and varying incubation time we could accurately determine the rate of repair ensuring that the assay was always in the linear phase when we performed the quantitative analysis.

3. Results

3.1. Differentiating mitotic SH-SY5Y cells into neuron-like postmitotic cells

For this research, it was critical to distinguish between neuroblasts that were simply nonproliferating and differentiated neurons that were postmitotic. Human SH-SY5Y neuroblastoma cells can be induced to differentiate into postmitotic neurons by manipulating culture conditions (Kulkarni et al., 2008). When grown in DMEM with 10% fetal bovine serum, SH-SY5Y cells are morphologically similar to fibroblasts (Fig. 1A, left panels). After incubation for 5 days in medium containing 10 μM retinoic acid, the cells begin to form neurites, although some cells continued to replicate. Subsequent use of medium containing BDNF resulted in at least 95% of the cells being postmitotic and exhibiting outgrowth of long neurites as seen by standard phase contrast microscopy (Fig. 1A, right panels).

To confirm that the morphologically differentiated cells have neuronal characteristics, we tested for expression of neuron-specific markers, including neuron-specific class III beta-tubulin (Tuj1), by standard immunocytochemistry techniques. Tuj1 stabilizes

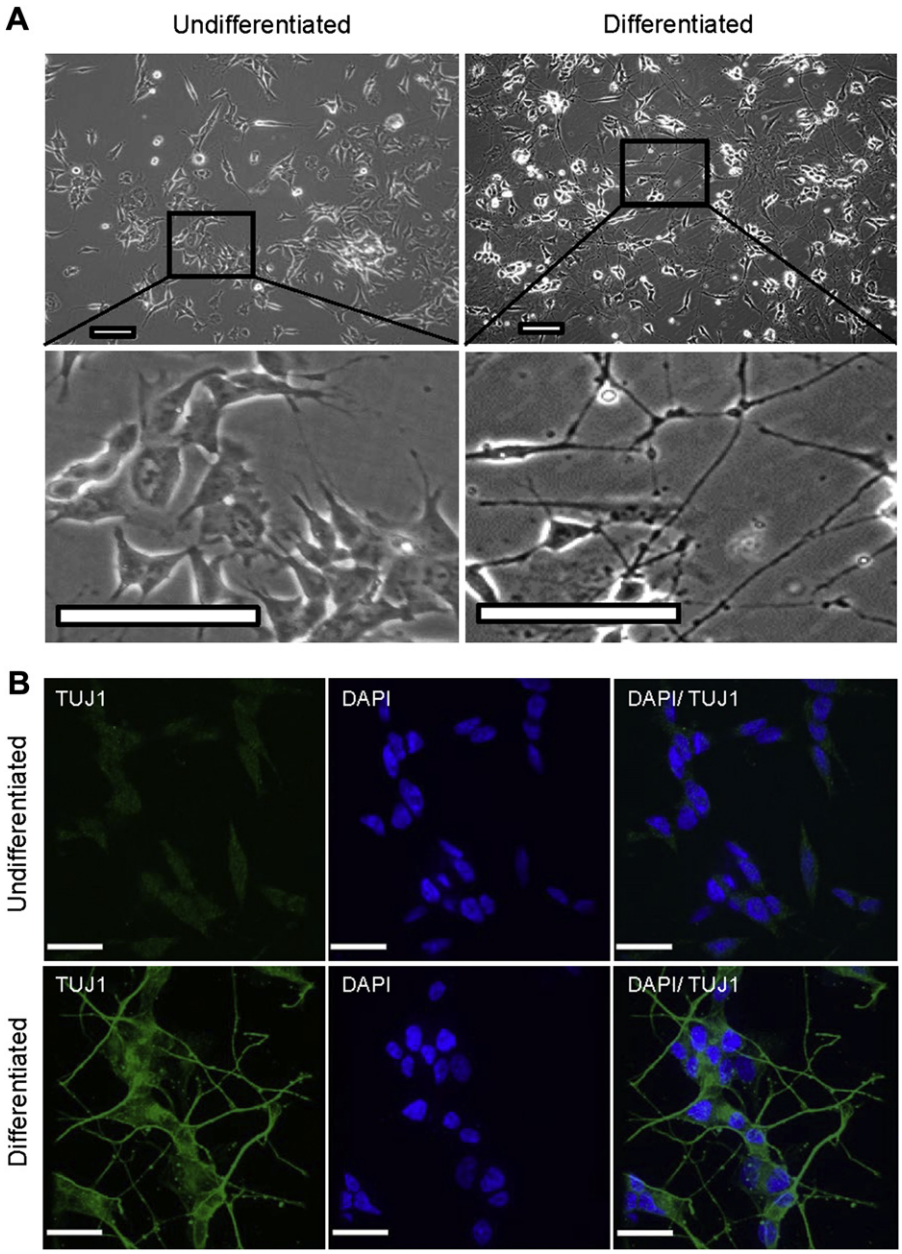

Fig. 1. Morphological change of SH-SY5Y cells differentiated from mitotic into postmitotic (neuron-like) cells. (A) Left panels, neuroblastoma cells before differentiation. Cells are treated with 10 μM retinoic acid for 5 days; at this time point some cells have extended short neurites but many cells are still dividing. Right panels, cells after an additional 5 days of culture in serum-free medium containing 10 ng/mL BDNF; at this time point most cells are postmitotic and exhibit long neurite formation. (B) The neuron-specific class III beta-tubulin (Tuj1) marker was present in the outgrowth axons of neurons after retinoic acid and BDNF treatment. In comparison untreated SH-SY5Y cells only showed light staining of Tuj1. Scale bar = 25 μM. Abbreviations: BDNF, brain-derived growth factor; DAPI, 4′,6′- diamidino-2-phenylindole.

microtubules in neuronal cell bodies and axons, and plays a role in axonal transport. The fully differentiated SH-SY5Y cells had Tuj1 immunoreactive axons, whereas this antibody labeling was weak or absent in undifferentiated cells (Fig. 1B). The Tuj1 image shows points of bright staining along the axons which we propose might be areas of protein aggregation. We also tested for the presence of an additional neuronal marker, microtubule-associated protein 2 (MAP2). MAP2 is believed to protect and stabilize newly formed microtubules and is a pertinent factor in neuronal development. Seen in Supplementary Fig. 1, only the postmitotic cells show any degree of MAP2 immunoreactivity. Using these well-established neuronal markers, we thus verified that the protocol used here with human SH-SY5Y neuroblastoma cells resulted in differentiation into postmitotic neuron-like cells.

3.2. Neurons can adequately repair damage caused by an alkylating agent

Previous research investigating the toxic effect of alkylating agents in the central nervous system has been largely restricted to murine and nonisogenic models. To establish whether the differentiation status of human neuroblastoma cells could influence sensitivity to DNA damaging agents, cells were exposed to the alkylating chemical, MMS. As graphed in Fig. 2A and B, we tested the vulnerability of undifferentiated and differentiated SH-SY5Y cells to a range of MMS concentrations. The cytotoxicity results presented in Fig. 2A show that after 4 hours of exposure to concentrations of MMS greater than 1 mM, there is a modest difference in survival between the two groups, significant at 1 mM

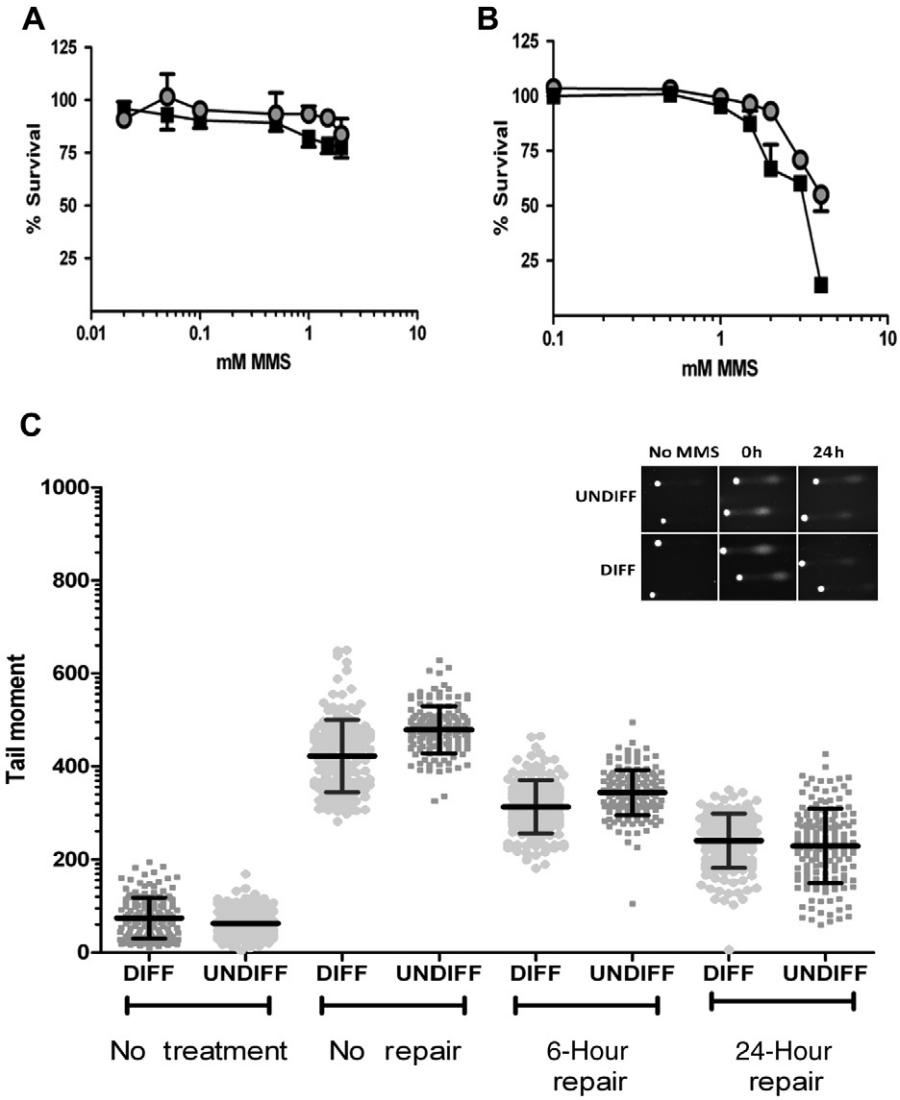

Fig. 2. MMS-induced DNA damage is repaired efficiently in differentiated and undifferentiated cells. (A) Cell survival after extended MMS exposure (4 hours). Cells were exposed to the indicated concentrations of MMS with survival measured using the WST-8 assay. (B) Cellular survival after a 1-hour MMS exposure and a 24-hour repair period using an LDH-based assay. ■ Denotes undifferentiated cells; ● denotes differentiated cells. All survival assays were repeated in triplicate. (C) Quantitative analysis of the tail moment after exposure to MMS. After 24 hours of repair both groups had comparable amounts of remaining DNA damage. The middle line in the scatter plot represents the mean ± SD. The comet assay was repeated in duplicate with consistent results. Graph inserts of representative comets images are shown. Abbreviations: DIFF, differentiated; LDH, lactate dehydrogenase; MMS, methyl methane sulfonate; UNDIFF, undifferentiated.

and 1.5 mM but not at 2 mM. Similar survival trends were also observed using an alternate treatment regime involving a 1-hour exposure at the indicated concentrations of MMS, followed by 24 hours of recovery (Fig. 2B).

We next used the alkali single-cell gel electrophoresis (comet) assay to determine the rate of DNA repair after MMS exposure. The assay here employed treatment with the DNA glycosylase Aag, which excises alkylated base modifications creating alkaline labile apurinic/apyrimidinic (AP) sites. Using this assay, the number of Aag-induced and also endogenous SSBs can be estimated from the length of the comet "tail" or moment (Fig. 2C, insert, and Supplementary Fig. 2). Initially, we determined the amount of endogenous damage present in both sets of cells (Fig. 2C, far left). Differentiated and undifferentiated cells without treatment had only low levels of endogenous DNA damage (Fig. 2C; Table 2).

To compare the rate of repair, both groups of cells were treated with 100 μM MMS for 1 hour, with comet tail length measured immediately after treatment and after periods of 6 or 24 hours of repair; all data points gathered are graphed in Fig. 2C and are summarized in Table 2. Immediately after MMS treatment, based on

Table 2
Numerical analysis of comet moment

	No treatment		No repair		6-Hour repair		24-Hour repair	
	DIFF	UNDIFF	DIFF	UNDIFF	DIFF	UNDIFF	DIFF	UNDIFF
MMS								
Mean	74	63	422	479	313	344	240	229
SD	44	28	78	51	57	49	58	80
Standard error	3	2	6	4	5	4	5	6
Number of values	161	159	146	147	144	169	151	158
H_2O_2								
Mean	69	55	703	752	487	563	346	270
SD	48	49	76	92	124	116	135	131
Standard error	5	5	10	12	11	12	12	14
Number of values	110	102	56	61	125	90	126	90

Key: DIFF, differentiated; MMS, methyl methane sulfonate; UNDIFF, undifferentiated.

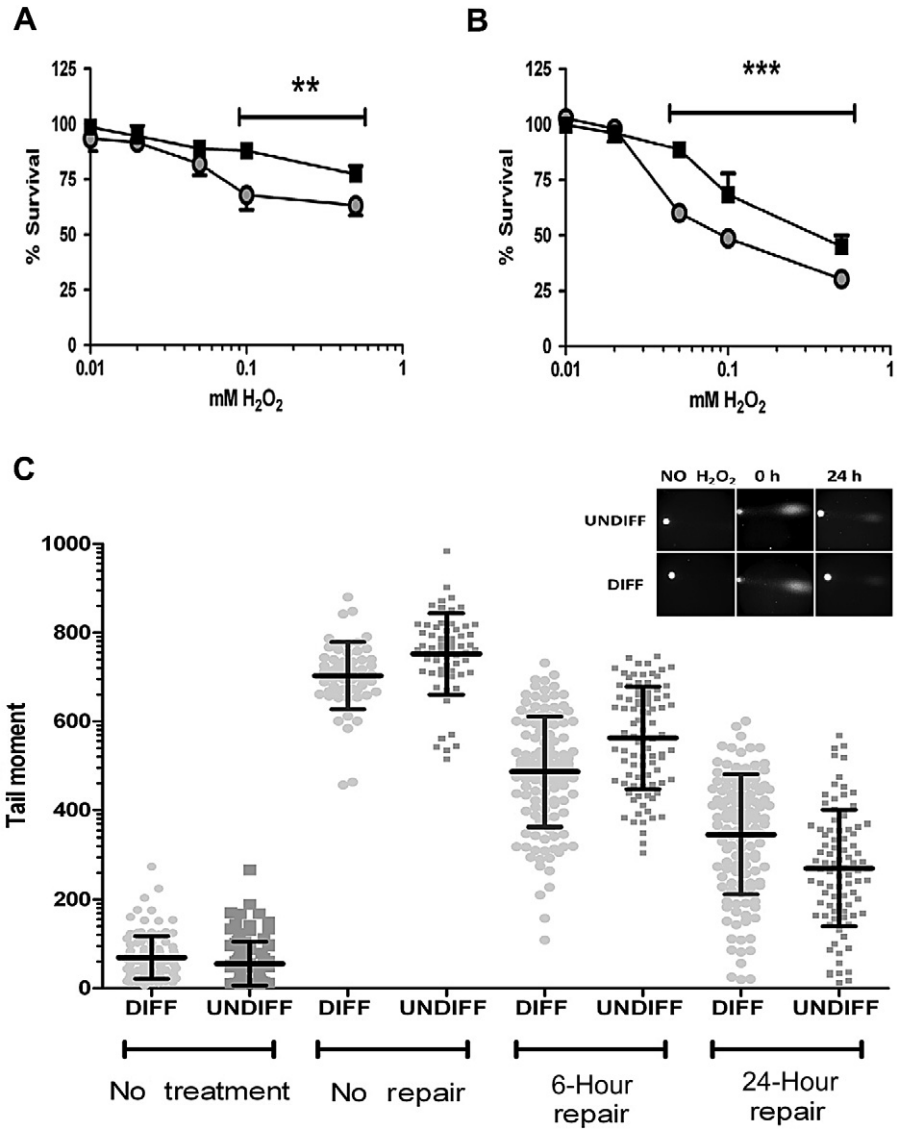

Fig. 3. Neuronal cells are more sensitive to oxidative DNA damage. (A) Cellular survival after extended (4-hour) exposure to H_2O_2 treatment. Survival was measured by WST-8 assay. (B) Cellular survival 24 hours after acute (40-minute) hydrogen peroxide treatment measured using an LDH-based assay. All survival assays were repeated in triplicate. ■ Denotes undifferentiated cells; ● denotes differentiated cells. ** $p < 0.05$, *** $p < 0.01$. (C) Analysis of the comet moment determined that undifferentiated cells had more DNA damage compared with differentiated cells after exposure to H_2O_2. However, 24 hours after exposure to H_2O_2 the undifferentiated cells had repaired more of the damage than differentiated cells. The middle line in the scatter plot represents the mean ± SD. Comet experiments were performed in duplicate. Graph inserts of representative comet images. Abbreviations: DIFF, differentiated; LDH, lactate dehydrogenase; UNDIFF, undifferentiated.

the results obtained from comparing the comet tails of 100 or more cells from both groups, undifferentiated cells (479 ± 51, arbitrary units) had accumulated a statistically higher ($p < 0.01$) amount of damage compared with differentiated cells (422 ± 78); we note that this analysis does not account for repair that might have taken place during the short period of exposure to MMS. DNA damage remained higher in undifferentiated cells after 6 hours of repair (344 ± 49 undifferentiated versus 313 ± 57 differentiated; $p < 0.01$), consistent with both groups repairing MMS-induced damage at a similar rate (28% of damage repaired in undifferentiated versus 26% in differentiated). Despite this, after 24 hours of repair the undifferentiated cells had repaired 52% of damage compared with only 44% for the differentiated group, resulting in both groups having comparable amounts of remaining damage ($p = 0.16$). Thus, the undifferentiated cells were more susceptible to the formation of MMS-induced lesions, yet appeared to repair this damage slightly more efficiently, resulting in similar amounts of remaining damage after 24 hours.

3.3. Neurons do not repair hydrogen peroxide-induced DNA damage efficiently

The comet and survival results described previously in this report support the notion that alkylating DNA damage is repaired effectively in cycling neuroblasts and postmitotic neuronal cells. To determine if neurons are particularly susceptible to oxidative DNA damage, we treated undifferentiated and differentiated cells with hydrogen peroxide at concentrations that cause oxidative DNA damage, including SSBs. Cellular survival after hydrogen peroxide exposure was tested as described earlier for MMS. After 4 hours of exposure, the differentiated cells were significantly more sensitive to hydrogen peroxide at concentrations greater than 100 μM, as

compared with undifferentiated cells (Fig. 3A). Further, after a 40-minute exposure and 24 hours of repair, low concentrations of hydrogen peroxide (50 μM) resulted in a noticeable difference in cellular survival, with the differentiated cells being significantly more sensitive to hydrogen peroxide damage than undifferentiated cells (Fig. 3B).

We used the comet assay to determine whether the increased sensitivity of the differentiated cells was because of reduced DNA repair capacity. For this assay, we used a low concentration of hydrogen peroxide, which caused significantly more cell death after 24 hours in the differentiated cells (50 μM). This time, the DNA glycosylase formamidopyrimidine DNA glycosylase was used to digest sites of oxidative damage and generate SSBs before comet analysis. Levels of endogenous DNA damage in both groups were found to be comparably low (Fig. 3C, far left; Table 2).

The DNA damage immediately after treatment caused by hydrogen peroxide was significantly higher ($p < 0.01$) in undifferentiated cells (752 ± 92 vs. 703 ± 76 in differentiated cells). After 6 hours of repair, the undifferentiated group had repaired approximately 25% of the initial damage, whereas the differentiated group had repaired 31%, resulting in the undifferentiated group still having significantly more remaining DNA damage ($p < 0.01$) (Table 2). In the 6- to 24-hour time frame, however, the undifferentiated cells repaired twice the amount of DNA damage as the differentiated cells. Hence, despite the undifferentiated cells accumulating more damage initially and having comparable levels of repair after 6 hours, these cells had a significantly lower ($p < 0.01$) amount of remaining DNA damage after 24 hours of repair. These data are consistent with the toxicity results showing that differentiated cells are more vulnerable to sustained DNA damage induced by 50 μM of hydrogen peroxide (Fig. 3B).

3.4. Modulation of SP-BER components in neuronally differentiated cells

SP-BER is regarded as the primary DNA repair mechanism for most forms of alkylative, oxidative, and SSB damage. Differences in BER capacity could reflect different levels of expression or differential activation of BER enzymes in undifferentiated and differentiated SH-SY5Y cells. This possibility was tested by performing immunoblot and enzyme activity assays on extracts from undifferentiated and differentiated cells. We consulted previous research using the SH-SY5Y cells from Castano and Kypt (2008) to carefully select the Western loading controls used in this study. We reproduced and then expanded on the previously published results and report that it is the retinoic acid treatments that affected the loading controls in the aforementioned study not necessarily the process of differentiation (Supplementary Fig. 3). Here we find that both β-actin and GAPDH loading controls gave comparable, reproducible results using extracts from undifferentiated and differentiated cells. We initially investigated BER activity and protein levels (Fig. 4A). There was no significant difference in levels of the DNA glycosylases OGG1 and UDG. However, core BER components APE1 ($p < 0.05$) and LIGIII ($p < 0.05$) were significantly decreased in differentiated neurons. XRCC1 protein was undetectable in the differentiated extracts. Previous preliminary studies using microarray analysis had indicated no significant change in XRCC1 transcript levels after differentiation of SY5Y neuroblastoma cells (referred to in Kulkarni et al., 2008); however in this study, our studies recapitulate the findings of Narciso and colleagues (Narciso et al., 2007), who found XRCC1 protein levels are significantly reduced upon differentiation. To more accurately determine XRCC1 transcript levels, real time reverse transcription polymerase chain reaction was conducted using RNA extracted from differentiated and undifferentiated cells. In Supplementary Fig. 4 we show that there is a significant downregulation of XRCC1 gene expression, however this did not correlate completely with the dramatic reduction in XRCC1 protein levels. These changes in BER enzyme levels between undifferentiated and differentiated cells caused a reduction in the SP-BER repair activity in the extracts from differentiated cells, measured using a substrate requiring both incorporation and ligation activity ($p < 0.05$) (Fig. 4B). The reduced SP-BER activity appeared independent of Pol β protein levels, however, did correlate with the reduction in XRCC1 protein levels. Further, we used the same substrate with the addition of T4 ligase to determine if there was an accumulation of ligatable intermediates indicating that ligase activity was potentially rate limiting (Supplementary Fig. 5). Indeed, in differentiated and undifferentiated extracts, the addition of T4 ligase resulted in an increase of DNA repair product. However, the amount of increase was far greater in the differentiated extracts suggesting that that these cells might be particularly deficient in ligation activity (Supplementary Fig. 5B). We expanded our investigation and measured individual enzymatic activities to more completely determine which activities associated with BER might be modulated by neural differentiation. In Fig. 4C, we show that total 8-oxoguanine incision activity (mainly a function of OGG1) is significantly decreased in the differentiated cells. UDG activity on a uracil opposite adenine (U:A) substrate is moderately increased, whereas the comparable activity on a uracil opposite guanine (U:G) substrate is slightly decreased (Fig. 4C). We also investigated the effect of differentiation on the 3 core enzymatic activities associated with SP-BER: AP site incision, single-nucleotide incorporation, and nick ligation (Fig. 4D). The decrease in total AP endonuclease activity in differentiated cells correlated with the reduction in APE1 protein levels. A reproducible decrease in incorporation activity was also observed in the differentiated group, a result that was surprising in light of the slightly increased Pol β protein level. Ligation activity in differentiated cells was reduced by approximately 90% (Fig. 4D), despite LIGIII protein levels decreasing by less than 25% (Fig. 4A).

3.5. Evidence that LP-BER activity is reduced in differentiated neurons

Though the results of the ligation assay did not reflect the LIGIII protein levels, the reduction in activity might be a result of reduced XRCC1 protein levels. Alternatively LIGI (which is primarily involved in LP-BER) would also be active on the nick substrate and might also influence the reduction in activity. Using immunoblot analysis, we determined that the LIGI protein level was substantially decreased (approximately 90%) in differentiated neurons (Fig. 5A). Considering that many other LP-BER proteins are involved in DNA replication, we investigated whether the nonreplicating status of the differentiated cells would modulate LP-BER protein levels. Indeed, FEN-1, Pol ε, and PCNA were all significantly reduced in postmitotic neurons compared with proliferating undifferentiated cells (Fig. 5A).

Next, we measured the effect of the dramatic decrease in LP-BER components on LP-BER activity. The LP-BER substrate we used contains a 5′ tetrahydrofuran (THF) group refractory to the deoxyribophosphodiesterase (dRP) activity of Pol β and requires processing by LP-BER. The previously reported weak retention of PCNA on linear substrates was circumvented by blocking both ends with a biotin-streptavidin conjugate, requiring PCNA to be loaded on and off the substrate (Fig. 5B, top). Because preliminary experiments showed that a high level of substrate degradation was present in the extracts from undifferentiated cells, we used lower protein concentrations to compare activity between the 2 groups.

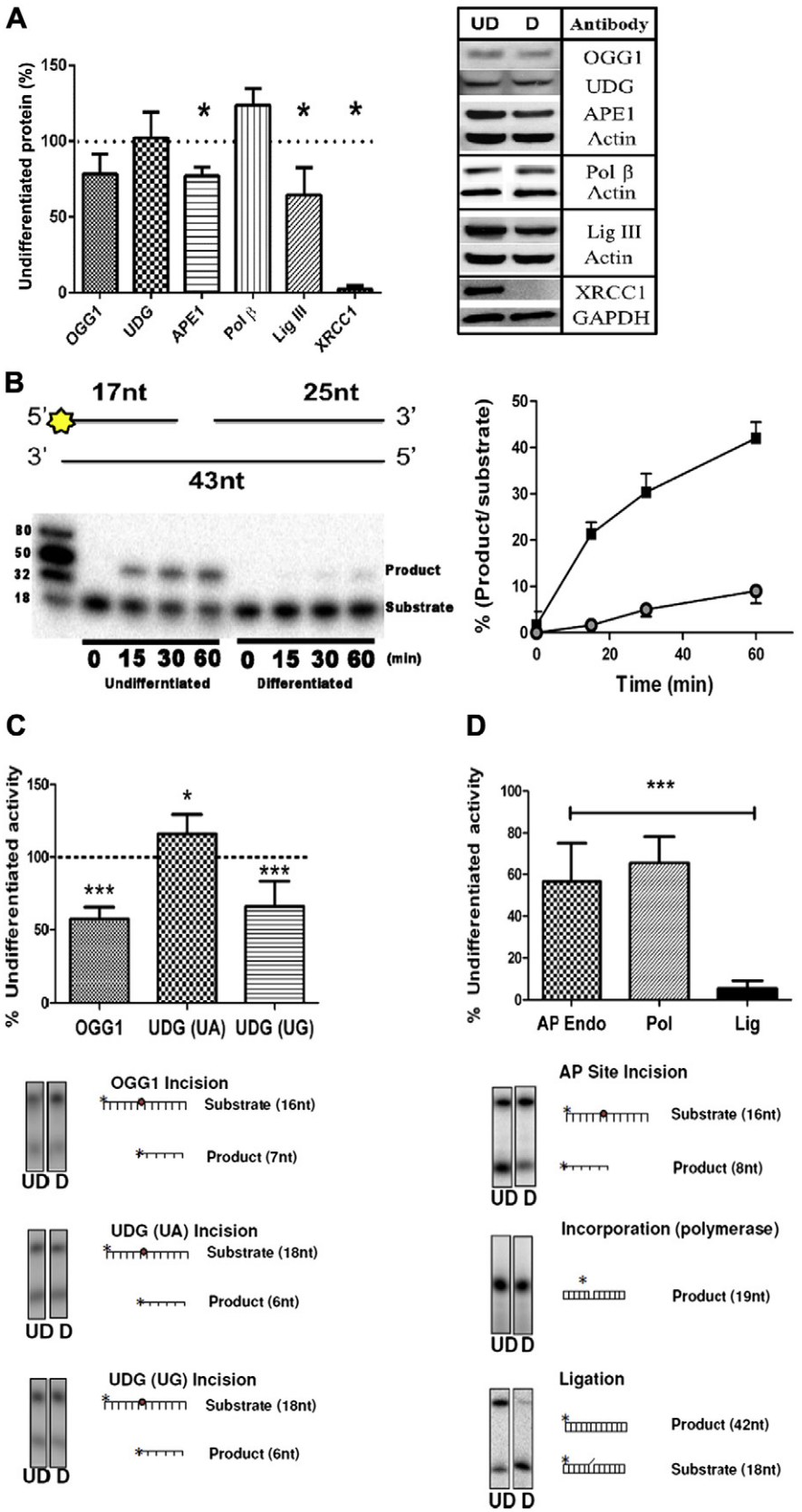

Fig. 4. Changes in SP-BER components and activity levels in differentiated cells. (A) Right panel: representative images from Western analysis. β-Actin was used as a loading control (* $p < 0.05$; $n = 4$). Left panel: protein levels of APE1 and Lig III were moderately yet significantly decreased after differentiation with only XRCC1 heavily decreased. (B) Right panel: SP-BER assay (top). Diagrammatic representation of oligonucleotide combination used in the assay. Star denotes 5′ radiolabeling site (refer to 2. Methods for additional information). Bottom: representative gel image from the SP-BER assay shows that there is robust SP-BER activity in the undifferentiated extracts; in contrast, differentiated extracts had greatly reduced activity (left panel). Undifferentiated cells have significantly higher levels of repair activity ($p < 0.01$) measured using a BER substrate incubated with 2 μg cell extract

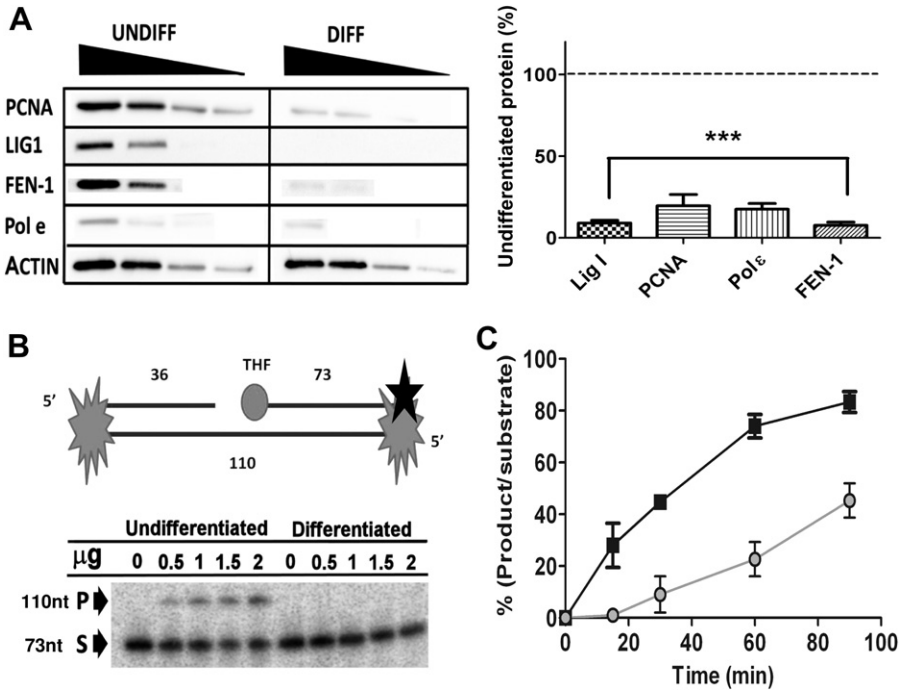

Fig. 5. Protein levels of LP-BER-associated proteins are heavily reduced in neurons resulting in a decrease in LP-BER capacity. (A) Left panel: representative Western blot using 80, 40, 20, and 10 μg of total protein extracts. Right panel: all LP-BER proteins investigated were significantly reduced after differentiation. *** $p < 0.01$; $n = 3$. (B) Upper: diagrammatic representation of LP-BER substrate (refer to 2. Methods for additional information). Black star denotes 3′ radiolabeling site. Lower panel: representative gel of LP-BER substrate using increasing total protein concentrations (0–2 μg) shows no LP-BER activity in differentiated extracts after a 15-minute incubation. (C) Time course for LP-BER assay shows that LP-BER activity in undifferentiated total cell extracts is significantly ($p < 0.01$; $n = 3$) higher at all time points investigated (■ denotes differentiated cells, ● denotes undifferentiated cells). Data are mean ± SD. Abbreviations: BER, base excision DNA repair; DIFF, differentiated; FEN-1, flap endonuclease-1; Lig, ligase; LP-BER, long patch BER; nt, nucleotide; P, product; PCNA, proliferating cell nuclear antigen; Pol, polymerase; S, substrate; THF, tetrahydrofuran; UNDIFF, undifferentiated.

As shown in Fig. 5B, after 30 minutes of incubation at a range of protein concentrations, LP-BER activity was only detected in extracts from the undifferentiated cells, consistent with the low protein levels for the integral LP-BER components in the differentiated cells (Fig. 5A). As shown in Fig. 5C, we also measured LP-BER activity over an extended period of 90 minutes, and our results indicate that LP-BER is approximately 4 times higher in undifferentiated cells compared with differentiated cells.

4. Discussion

The goal of this study was to evaluate how neuronal cell differentiation affects BER efficiency and the response to DNA damage. Using SH-SY5Y neuroblastoma cells as a model, we observed that replicating cells treated with hydrogen peroxide or MMS show a higher capacity to repair DNA damage and also, a higher level of expression of BER proteins and activities. One of the central assertions of this study is that BER components are modulated according to the differentiation status of the neuron. We make this assertion based on the results of 8 distinct quantitative biochemical assays, measuring a total of 12 different types of DNA repair. In each case the assay produced highly reproducible results which, when coupled with extensive Western analysis on the proteins involved in both SP- and LP-BER allowed us to confidently determine that after neuronal differentiation SP-BER repair is reduced because of a decrease in XRCC1 and Ligase I. Despite this reduction, LP-BER does not compensate, decreasing dramatically because of a reduction in LP-BER components associated with replication. We find that despite the postmitotic cells not being more sensitive to alkylating damage, they are prone to cellular toxicity induced by oxidative stress, apparently because of an impaired ability to repair the associated DNA damage.

One possible explanation for the observed increased vulnerability of genomic DNA in undifferentiated cells is that actively replicating chromatin is especially susceptible to DNA damage. Consistent with this hypothesis, previous studies from our group demonstrated that Chinese hamster ovary cells were hypersensitive to ultraviolet irradiation during S-phase (Orren et al., 1997; Petersen et al., 1995). Thus, chromatin of undifferentiated cells, which is maintained in an open conformation to facilitate active DNA replication and transcription, is more available for modification by exogenous DNA damaging agents (Bubley et al., 1996). Notably, Bill et al. reported results that are consistent with the present study, including that undifferentiated mesenchymal stem cells have a higher DNA repair rate in actively transcribed genes and a higher DNA repair efficiency than terminally differentiated cells (Bill et al., 1991). Moreover, 2 recent studies reported that the speed of DNA repair depends on the relaxed or compacted state of chromatin (Amouroux et al., 2010; Mosesso et al., 2010). Of note, the work presented here focuses primarily on repair in the nucleus, however, many of the enzymes involved in nuclear DNA repair are also associated with mitochondrial DNA repair (reviewed in Sykora

(■ denotes undifferentiated cells, ● denotes differentiated cells). The assay was conducted in triplicate. Data are mean ± SD. (C) Activities of OGG1, UDG (U:G) were significantly decreased after cellular differentiation (*** $p < 0.01$, * $p < 0.05$). (D) Core BER activities are decreased in differentiated cells. Incision and incorporation activity was moderately decreased. In contrast, ligation activity is heavily reduced in neurons. (*** $p < 0.01$, conducted at least in triplicate). In all panels the mean ± SD is plotted. Abbreviations: AP, apurinic/apyrimidinic site; APE1, AP endonuclease 1 (APE1); BER, base excision DNA repair; D, differentiated; Endo, endonuclease; Lig, Ligase; nt, nucleotide; OGG1, 8-oxoguanine glycosylase 1; Pol, Polymerase; SP-BER, short patch BER; U, uracil; UA, uracil:adenine; UD, undifferentiated; UDG, uracil DNA glycosylase; UG, uracil:guanine.

et al., 2012). It remains to be tested whether the repair of mitochondrial damage is also decreased after differentiation and how this affects cellular survival after genotoxic stress.

Our data indicate that ligation activity is particularly affected in postmitotic neurons and suggest that the reduced ligation is a direct effect of a pronounced decrease in LIGI levels. A decrease in LIGI protein levels has also been reported in nonneural human cell models, including terminally differentiated muscle cells (Narciso et al., 2007) and nonproliferating keratinocytes (Krokan et al., 1997), suggesting that the result might be indicative of a nonproliferating cell regardless of differentiation status. Importantly, in all of these reports, including our own, LIGI protein is not completely absent, but greatly reduced. This corroborates early reports (Montecucco et al., 1992) describing that ligase I mRNA was detected at low levels in a number of nonproliferating cell types, including mature rat neurons, further supporting the involvement of this enzyme in DNA repair in differentiated cells.

The functional redundancy of ligases in DNA repair is of particular interest in neurons considering the low levels of LIGI. In recent work by Gao et al. LIGIII was shown to be dispensable in the nucleus, but not in the mitochondria, in cells from the murine nervous system (Gao et al., 2011). This exchangeability is also supported by work conducted by Sleeth et al. (2004), who demonstrated the ability of LIGI to participate in SP- and LP-BER, and that LIGIII participated exclusively in SP-BER. Here, we show that human neuronal cells are not particularly sensitive to MMS. Our data suggest that alkylating damage is largely unaffected by the reduced LIGI protein levels. This notion is strengthened by data from Bentley et al. (2002) showing that the ethyl methane sulfonate survival curve for Ligase I null mouse fibroblasts was indistinguishable from the wild type mouse control. Despite previous reports that LIGI participates in SP-BER, it does not appear to be required for the repair of alkylating damage in neuronal cells.

An important contribution of this work is that it clearly shows that neurons are particularly susceptible to agents that induce oxidative DNA damage. This might be in part attributed to reduced levels of OGG1-related activity, because neurons from OGG1-deficient mice exhibit increased vulnerability to oxidative stress (Liu et al., 2011). However, this heightened sensitivity is unlikely to be caused by a breakdown in any of the core SP-BER components (APE1, Pol β, LIGIII), considering these cells efficiently repair alkylating damage. Instead, it might be related to the spectrum of DNA damage produced by oxidizing agents.

Oxidative damage can result in direct DNA damage, such as 8-oxo-G lesions, but can also generate significant amounts of SSBs. Though SSBs with simple 3′-hydroxyl and 5′-phosphate ends are substrates for SP-BER, many 5′ modifications that are refractory to Pol β dRP lyase activity require LP-BER. We show that neuronal differentiation is coupled with a decrease in LP-BER proteins FEN-1, PCNA, Pol ε, and LIGI, resulting in a severely reduced BER capacity. In support of our data, Wei and Englander (2008) recently looked at differences in BER processing in mitotic and proliferating tissue and found that LP-BER capacity for a 5′ blocking group was nearly 6-fold lower in brain samples compared with proliferating intestinal mucosa. Though comparing DNA repair capacity across different tissue types should be approached with caution, these results are similar to some in this study and suggest that repair of 5′ blocking groups in the brain is particularly poor. Furthermore, the severe progressive cerebellar ataxia associated with ataxia with ocular motor apraxia 1 (AOA1) is evidence that reduced repair of 5′ blocking groups is particularly deleterious in the brain. AOA1 is caused by mutations in aprataxin (*APTX*), a protein responsible for resolving 5′-adenosine monophosphate (5′-AMP) ligation intermediates. The predominant neural specificity of the disorder might stem from a lack of backup DNA repair mechanisms available to replicating cells. Here we report that LP-BER, a potential backup repair mechanism for the 5′-AMP in the absence of aprataxin, is severely reduced in neurons and this might contribute to the neural specificity of AOA1.

The brain requires large amounts of oxygen to sustain high levels of metabolic activity in neuronal and associated cells. This activity invariably produces ROS with the potential to cause oxidative damage. Normally, however, BER can be upregulated in response to excitation of neurons, as was recently shown in cultured rat cerebral cortical neurons where activation of glutamate receptors induced the expression of APE1 and enhanced BER (Yang et al., 2010). Many neurodegenerative disorders are associated with an increase in oxidative stress and impaired DNA repair. Loss of BER capacity may contribute to the accumulation of DNA damage reported to occur in vulnerable populations of neurons in several neurodegenerative disorders, including Alzheimer's disease (Moreira et al., 2008; Weissman et al., 2007), Parkinson disease (Nakabeppu et al., 2007; Yang et al., 2008), Huntington disease (Trushina and McMurray, 2007), and amyotrophic lateral sclerosis (Aguirre et al., 2005). Interestingly, brain cells of Alzheimer's disease patients show significant BER dysfunction and reduced expression of UDG and OGG1 activities (Weissman et al., 2007). We propose that loss of BER capacity in terminally differentiated neurons could cause persistent DNA damage to accumulate over time. This higher level of DNA damage might be more readily tolerated in a nonreplicating cell than in a replicating cell, in which persistent DNA damage activates cell cycle checkpoints, such as those mediated by ataxia telangiectasia mutated (ATM)/ ataxia telangiectasia and Rad3-related protein (ATR) and P53, and triggers cell death (Kruman et al., 2004). Without this cell cycle signaling in differentiated neurons, DNA damage can accumulate and impair function, a process observed in normal aging and this might be more severe in the dysfunctional BER background of neurodegenerative diseases.

Disclosure statement

The authors report no conflicts of interest.

Acknowledgements

The authors thank Dr Robert Bambara for reagents provided, and Dr Misiak and Dr Illuzzi for critical reading of the manuscript. This research is supported by intramural research program of National Institute on Aging, National Institutes of Health.

Appendix A. Supplementary data

Supplementary data associated with this article can be found, in the online version, at http://dx.doi.org/10.1016/j.neurobiolaging.2012.12.016.

References

Aguirre, N., Beal, M.F., Matson, W.R., Bogdanov, M.B., 2005. Increased oxidative damage to DNA in an animal model of amyotrophic lateral sclerosis. Free Radic. Res. 39, 383–388.

Amouroux, R., Campalans, A., Epe, B., Radicella, J.P., 2010. Oxidative stress triggers the preferential assembly of base excision repair complexes on open chromatin regions. Nucleic Acids Res. 38, 2878–2890.

Aprelikova, O.N., Tomilin, N.V., 1982. Activity of uracil-DNA glycosylase in different rat tissues and in regenerating rat liver. FEBS Lett. 137, 193–195.

Bentley, D.J., Harrison, C., Ketchen, A.M., Redhead, N.J., Samuel, K., Waterfall, M., Ansell, J.D., Melton, D.W., 2002. DNA ligase I null mouse cells show normal DNA repair activity but altered DNA replication and reduced genome stability. J. Cell Sci. 115, 1551–1561.

Bill, C.A., Grochan, B.M., Meyn, R.E., Bohr, V.A., Tofilon, P.J., 1991. Loss of intragenomic DNA repair heterogeneity with cellular differentiation. J. Biol. Chem. 266, 21821–21826.

Bubley, G.J., Xu, J., Kupiec, N., Sanders, D., Foss, F., O'Brien, M., Emi, Y., Teicher, B.A., Patierno, S.R., 1996. Effect of DNA conformation on cisplatin adduct formation. Biochem. Pharmacol. 51, 717–721.

Castano, Z., Kypt, R., 2008. Housekeeping proteins: limitations as references during neuronal differentiation. The Open Neuroscience Journal 2, 36–40.

Englander, E.W., 2008. Brain capacity for repair of oxidatively damaged DNA and preservation of neuronal function. Mech. Ageing Dev. 129, 475–482.

Frosina, G., Fortini, P., Rossi, O., Carrozzino, F., Raspaglio, G., Cox, L.S., Lane, D.P., Abbondandolo, A., Dogliotti, E., 1996. Two pathways for base excision repair in mammalian cells. J. Biol. Chem. 271, 9573–9578.

Gao, Y., Katyal, S., Lee, Y., Zhao, J., Rehg, J.E., Russell, H.R., McKinnon, P.J., 2011. DNA ligase III is critical for mtDNA integrity but not Xrcc1-mediated nuclear DNA repair. Nature 471, 240–244.

Haug, T., Skorpen, F., Aas, P.A., Malm, V., Skjelbred, C., Krokan, H.E., 1998. Regulation of expression of nuclear and mitochondrial forms of human uracil-DNA glycosylase. Nucleic Acids Res. 26, 1449–1457.

Hildrestrand, G.A., Diep, D.B., Kunke, D., Bolstad, N., Bjoras, M., Krauss, S., Luna, L., 2007. The capacity to remove 8-oxoG is enhanced in newborn neural stem/progenitor cells and decreases in juvenile mice and upon cell differentiation. DNA Repair (Amst.) 6, 723–732.

Jensen, L., Linn, S., 1988. A reduced rate of bulky DNA adduct removal is coincident with differentiation of human neuroblastoma cells induced by nerve growth factor. Mol. Cell. Biol. 8, 3964–3968.

Jonsson, Z.O., Hindges, R., Hubscher, U., 1998. Regulation of DNA replication and repair proteins through interaction with the front side of proliferating cell nuclear antigen. EMBO J. 17, 2412–2425.

Krokan, H.E., Standal, R., Slupphaug, G., 1997. DNA glycosylases in the base excision repair of DNA. Biochem. J. 325, 1–16.

Kruman, I.I., Wersto, R.P., Cardozo-Pelaez, F., Smilenov, L., Chan, S.L., Chrest, F.J., Emokpae Jr.., R., Gorospe, M., Mattson, M.P., 2004. Cell cycle activation linked to neuronal cell death initiated by DNA damage. Neuron 41, 549–561.

Kulkarni, A., McNeill, D.R., Gleichmann, M., Mattson, M.P., Wilson III., D.M., 2008. XRCC1 protects against the lethality of induced oxidative DNA damage in nondividing neural cells. Nucleic Acids Res. 36, 5111–5121.

Liu, D., Croteau, D.L., Souza-Pinto, N., Pitta, M., Tian, J., Wu, C., Jiang, H., Mustafa, K., Keijzers, G., Bohr, V.A., Mattson, M.P., 2011. Evidence that OGG1 glycosylase protects neurons against oxidative DNA damage and cell death under ischemic conditions. J. Cereb. Blood Flow Metab. 31, 680–692.

Martin, L.J., 2008. DNA damage and repair: relevance to mechanisms of neurodegeneration. J. Neuropathol. Exp. Neurol. 67, 377–387.

Montecucco, A., Biamonti, G., Savini, E., Focher, F., Spadari, S., Ciarrocchi, G., 1992. DNA ligase I gene expression during differentiation and cell proliferation. Nucleic Acids Res. 20, 6209–6214.

Moreira, P.I., Nunomura, A., Nakamura, M., Takeda, A., Shenk, J.C., Aliev, G., Smith, M.A., Perry, G., 2008. Nucleic acid oxidation in Alzheimer disease. Free Radic. Biol. Med. 44, 1493–1505.

Morris, E.J., Dreixler, J.C., Cheng, K.Y., Wilson, P.M., Gin, R.M., Geller, H.M., 1999. Optimization of single-cell gel electrophoresis (SCGE) for quantitative analysis of neuronal DNA damage. Biotechniques 26, 282–289.

Mosesso, P., Palitti, F., Pepe, G., Pinero, J., Bellacima, R., Ahnstrom, G., Natarajan, A.T., 2010. Relationship between chromatin structure, DNA damage and repair following X-irradiation of human lymphocytes. Mutat. Res. 701, 86–91.

Nakabeppu, Y., Tsuchimoto, D., Yamaguchi, H., Sakumi, K., 2007. Oxidative damage in nucleic acids and Parkinson's disease. J. Neurosci. Res. 85, 919–934.

Narciso, L., Fortini, P., Pajalunga, D., Franchitto, A., Liu, P., Degan, P., Frechet, M., Demple, B., Crescenzi, M., Dogliotti, E., 2007. Terminally differentiated muscle cells are defective in base excision DNA repair and hypersensitive to oxygen injury. Proc. Natl. Acad. Sci. U. S. A. 104, 17010–17015.

Orren, D.K., Petersen, L.N., Bohr, V.A., 1997. Persistent DNA damage inhibits S-phase and G2 progression, and results in apoptosis. Mol. Biol. Cell 8, 1129–1142.

Petersen, L.N., Orren, D.K., Bohr, V.A., 1995. Gene-specific and strand-specific DNA repair in the G1 and G2 phases of the cell cycle. Mol. Cell. Biol. 15, 3731–3737.

Raymond, A.C., Staker, B.L., Burgin Jr., A.B., 2005. Substrate specificity of tyrosyl-DNA phosphodiesterase I (Tdp1). J. Biol. Chem. 280, 22029–22035.

Sleeth, K.M., Robson, R.L., Dianov, G.L., 2004. Exchangeability of mammalian DNA ligases between base excision repair pathways. Biochemistry 43, 12924–12930.

Sykora, P., Wilson III., D.M., Bohr, V.A., 2012. Repair of persistent strand breaks in the mitochondrial genome. Mech. Ageing Dev. 133, 169–175.

Takahashi, T., Tada, M., Igarashi, S., Koyama, A., Date, H., Yokoseki, A., Shiga, A., Yoshida, Y., Tsuji, S., Nishizawa, M., Onodera, O., 2007. Aprataxin, causative gene product for EAOH/AOA1, repairs DNA single-strand breaks with damaged 3′-phosphate and 3′-phosphoglycolate ends. Nucleic Acids Res. 35, 3797–3809.

Trushina, E., McMurray, C.T., 2007. Oxidative stress and mitochondrial dysfunction in neurodegenerative diseases. Neuroscience 145, 1233–1248.

Wei, W., Englander, E.W., 2008. DNA polymerase beta-catalyzed-PCNA independent long patch base excision repair synthesis: a mechanism for repair of oxidatively damaged DNA ends in post-mitotic brain. J. Neurochem. 107, 734–744.

Weissman, L., de Souza-Pinto, N.C., Mattson, M.P., Bohr, V.A., 2009. DNA base excision repair activities in mouse models of Alzheimer's disease. Neurobiol. Aging 30, 2080–2081.

Weissman, L., Jo, D.G., Sorensen, M.M., de Souza-Pinto, N.C., Markesbery, W.R., Mattson, M.P., Bohr, V.A., 2007. Defective DNA base excision repair in brain from individuals with Alzheimer's disease and amnestic mild cognitive impairment. Nucleic Acids Res. 35, 5545–5555.

Whitehouse, C.J., Taylor, R.M., Thistlethwaite, A., Zhang, H., Karimi-Busheri, F., Lasko, D.D., Weinfeld, M., Caldecott, K.W., 2001. XRCC1 stimulates human polynucleotide kinase activity at damaged DNA termini and accelerates DNA single-strand break repair. Cell 104, 107–117.

Yang, J.L., Tadokoro, T., Keijzers, G., Mattson, M.P., Bohr, V.A., 2010. Neurons efficiently repair glutamate-induced oxidative DNA damage by a process involving CREB-mediated up-regulation of apurinic endonuclease 1. J. Biol. Chem. 285, 28191–28199.

Yang, J.L., Weissman, L., Bohr, V.A., Mattson, M.P., 2008. Mitochondrial DNA damage and repair in neurodegenerative disorders. DNA Repair (Amst.) 7, 1110–1120.